Interspecies Differences in the Life Span Distribution: Humans versus Invertebrates

SHIRO HORIUCHI

Life span varies considerably among species. Investigation of reasons for interspecies differences in the length of life deepens our fundamental understanding of senescence and longevity.

A statistic frequently used for interspecies comparison of life span is the longest length of life ever documented reliably for each species (Carey and Judge 2000; Comfort 1979). Measures of the typical length of life such as the mean, median, and modal ages at death are also compared among populations of different species.

Information on the maximum length and typical length of life should be used carefully, however, taking into account the *distribution* of life span in the population. In some species, life spans may concentrate in a relatively narrow age range, while in others life spans may spread widely. In some species, the maximum length may not appear too far from the typical length, while in others the longest record may be an extreme exception.

To study the life span distribution in detail, data are needed on deaths by age in a large-size cohort of several thousand or more individuals. Until around 1990, survival data on large-size cohorts were rare except for humans. Thanks to the development of biodemography, however, survival data on large cohorts were obtained for several animal species in the 1990s (Vaupel et al. 1998) and such work is continuing. These data sets provide valuable opportunities for interspecies comparison of life span distribution.

The data were collected for laboratory animals, which live in protected environments. Such animals are substantially more protected from predators, infections, food shortages, climate changes, toxic materials, and accidental injuries than animals in the natural world. Also, modern humans usually live in more protected environments than our ancestors in prehistoric eras. The majority of deaths of adult individuals in protected environ-

ments are likely to result from diseases that are related to age-associated declines in physiological conditions.[1]

Therefore, the life span distribution in a protected population should reflect two crucial aspects of longevity. First, the distribution is affected by individual differences in the level of somatic maintenance. Greater individual variations in durability of physiological systems may produce a wider dispersion in the length of life. Second, the life span distribution is affected by age-related physiological changes in individuals. In populations in which physiological conditions deteriorate more rapidly, the death rate is likely to rise more steeply, thereby making the peak of life span distribution higher. These two sources of life span distribution correspond to two major dimensions of physiological variations: physiological differences *among individuals* of the same age and physiological changes *with age* in individuals. In summary, interspecies differences in the life span distribution in protected environments permit comparison of species with respect to (1) the size of individual variation in the ability to keep the organism functioning and (2) the trajectory of age-related changes in physiological conditions.[2]

Several researchers found interspecies similarities in the age patterns of mortality among animal species. The Gompertz equation was fitted to survival data for a number of species (Finch 1990; Finch and Pike 1996). The shapes of survival curves derived from intrinsic mortality data were shown to be similar for three mammalian species: dogs, mice, and humans (Carnes, Olshansky, and Grahn 1996). The age-related mortality increase slows down or ceases at very old ages in a number of species (Vaupel et al. 1998).

In this chapter, the focus is shifted from interspecies similarities to differences. Life span distributions of six cohorts of different species are compared, their major differences are identified, and possible explanations of the differential patterns are proposed.

Data and methods

Six species were compared: humans, Mediterranean fruit flies or "medflies" (*Ceratitis capitata*), nematode worms (*Caenorhabditis elegans*), parasitoid wasps (*Diachasmimorpha longjacaudtis*), another fruit fly species (*Drosophila melanogaster*), and bean beetles (*Callosobruchus maculatus*). The five nonhuman species are invertebrates.

Life tables were obtained for 347,533 individuals born in Sweden in 1881–85; 598,118 medflies; about 550,000 nematodes; 13,358 wasps; 5,245 *Drosophila* fruit flies; and 829 beetles.[3] All of them were males except the nematodes, which were hermaphrodites.[4] The nematode cohort and *Drosophila* cohort were inbred lines, thus genetically homogeneous. (Details on the data are given in Appendix A.)

The six cohorts were compared with respect to three life table functions: the life span distribution, the age-specific death rate, and the life table aging rate. Life span differs greatly among species. Therefore, it is more reasonable to compare the life span distribution *relative to the typical life span* than on the absolute time scale (days or years). The modal life span was used as the typical length of life.[5] The modal life span is useful in studies of senescence and longevity because it is determined by adult mortality only.[6] The mean and median life spans can be strongly affected by mortality at young ages, and should not be used for comparing species that have very different patterns of birth and neonatal mortality.[7] Life table functions were rescaled using one-hundredth of the modal life span as the time unit, instead of a day or year.[8] After the rescaling, all species appear to have the same modal life span.

In addition, the data were analyzed using mathematical models called frailty models. The analysis produces estimates of (1) the size of individual variation in vulnerability to mortality risk and (2) the age pattern of mortality risk at the individual level. (See Appendix B for discussion of the statistical methods.)

Differences in the life span distribution

Figures 1, 2, and 3 display the life span distribution, age-specific death rates, and life table aging rates, respectively, for the six species. Dots indicate observed values, and solid lines show estimates by mathematical models. In each panel, the modal life span in the cohort is placed at the same location, indicated by the dotted vertical line.

Figure 1 shows two major differences between humans and invertebrates. First, the distribution is skewed to the left in humans, but is fairly symmetrical around the mode in invertebrates.[9] Second, the relative variation of life span is smaller in humans than in vertebrates. The variability differs between invertebrates as well. The dispersion is smaller in nematodes, *Drosophila*, and beetles than in medflies and wasps.

The life span distribution is uniquely determined by age-specific death rates. It has been shown for different species that the death rate tends to rise steeply with adult age, then to slow down at old ages (Vaupel et al. 1998). A series of simulations (described in Appendix C) suggests the following relationships between mortality pattern and life span distribution. A steeper age-associated increase of mortality concentrates deaths in a narrower age range, thereby raising the peak of life span distribution. Mortality deceleration weakens this effect, but to a lesser extent if the slowing down starts later. In addition, the delayed mortality deceleration shifts the peak of life span distribution to an older age, leaving fewer survivors beyond the peak age and skewing the distribution more to the left. Figures 2

FIGURE 1 The life span distribution for six species

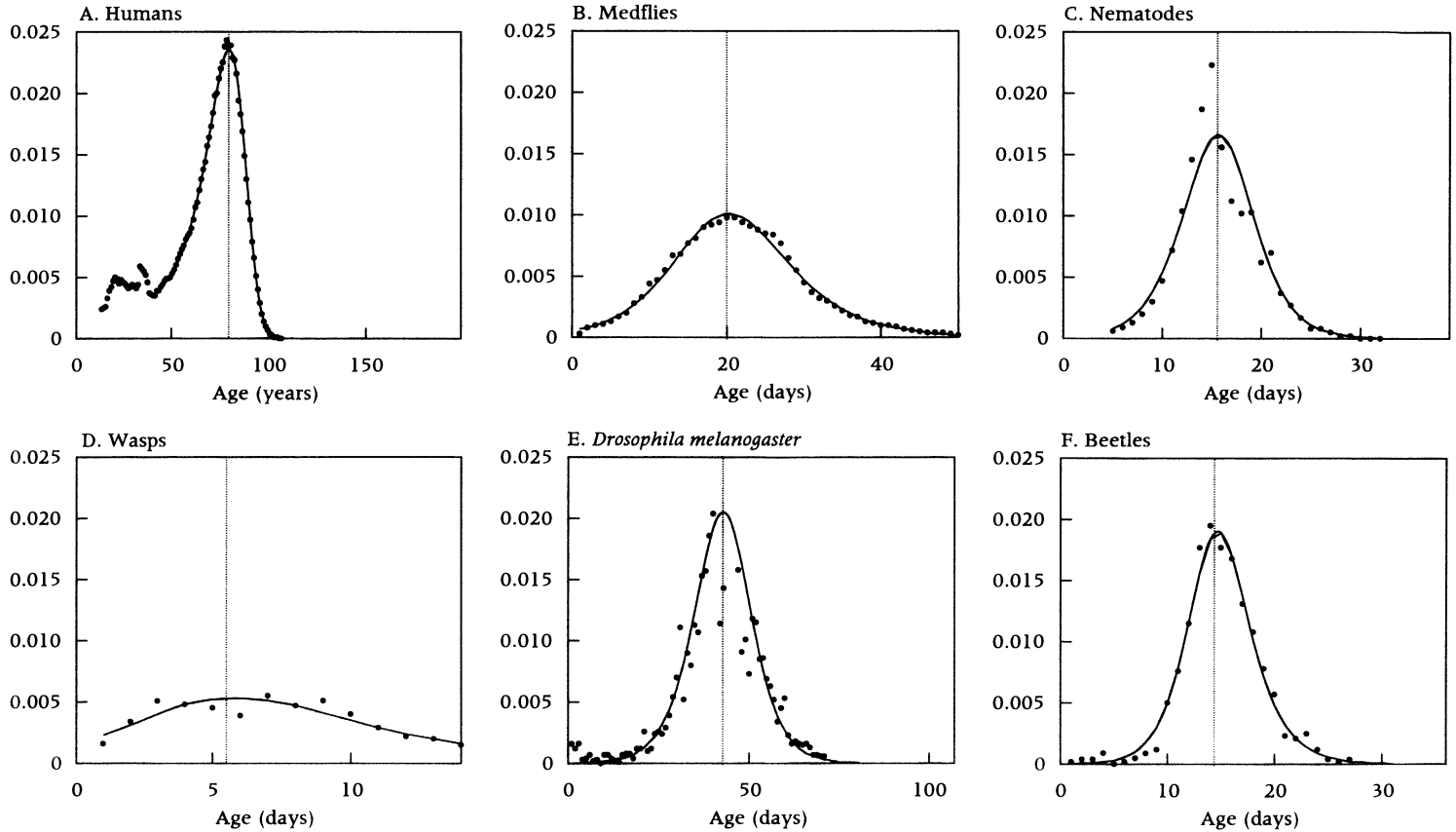

NOTE: Dots indicate values directly calculated from data, and solid lines indicate estimates using frailty models. In each panel, the vertical dotted line indicates the estimated modal life span, the vertical axis indicates the proportion of adult deaths per one-hundredth of the modal life span, and the area under the curve over the adult age range (defined in Appendix A) is unity if the age is rescaled to make the modal life span 100.

SOURCES: Humans, Swedish males born in 1881–85, from Berkeley Mortality Database (http://www.demog.berkeley.edu/wilmoth/mortality/); medflies, Carey et al. 1995, appendix; beetles, generation 1 males, Tatar and Carey 1994, Table 1; the other species, Vaupel et al. 1998, Figure 3.

FIGURE 2 Age-specific death rates for six species

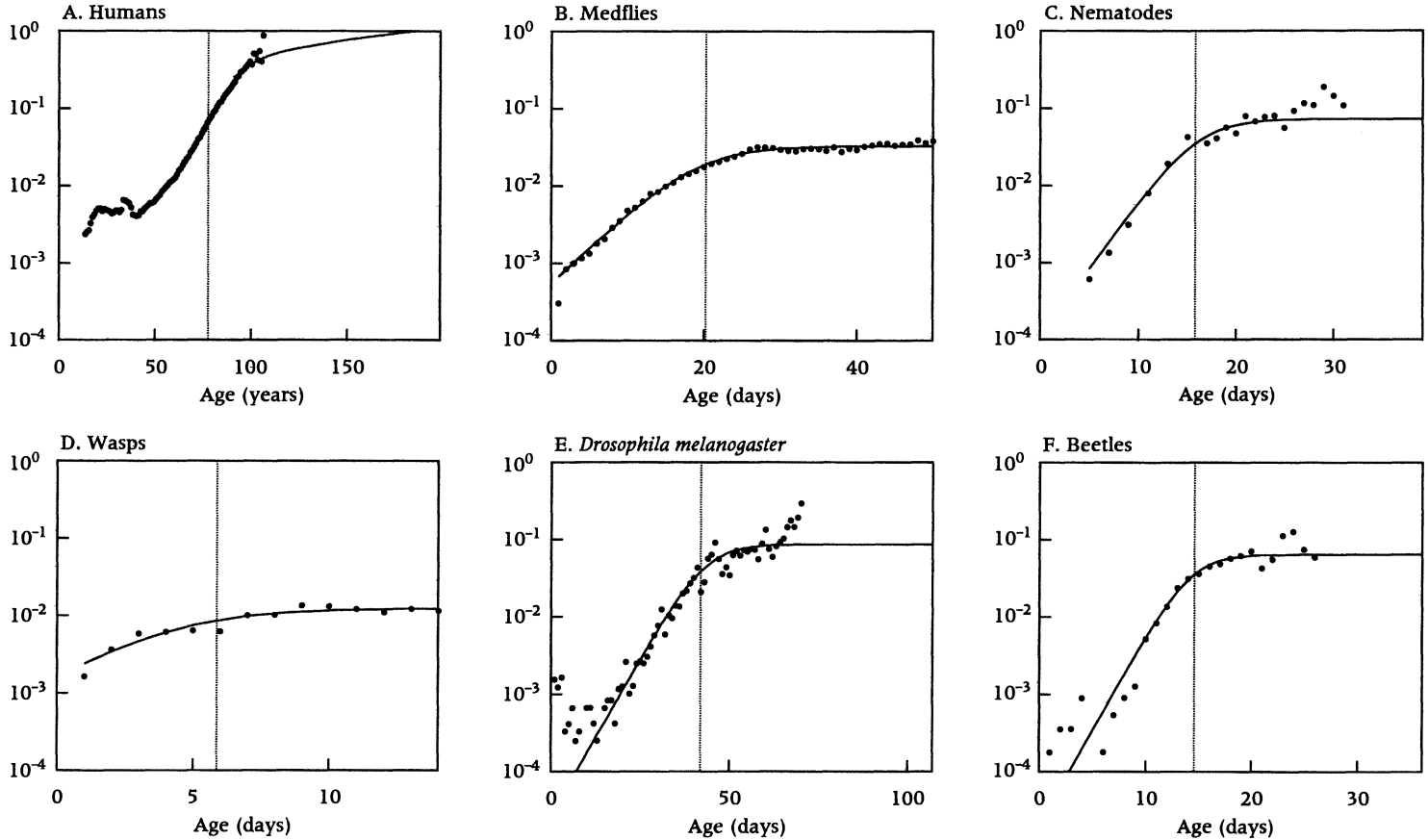

NOTE: Dots indicate values directly calculated from data, and solid lines indicate estimates using frailty models. In each panel, the vertical dotted line indicates the estimated modal life span, and the vertical axis indicates the number of deaths per individual-OHM of exposure. (OHM is one-hundredth of the modal life span.)
SOURCES: See Figure 1.

FIGURE 3 Life table aging rates for six species

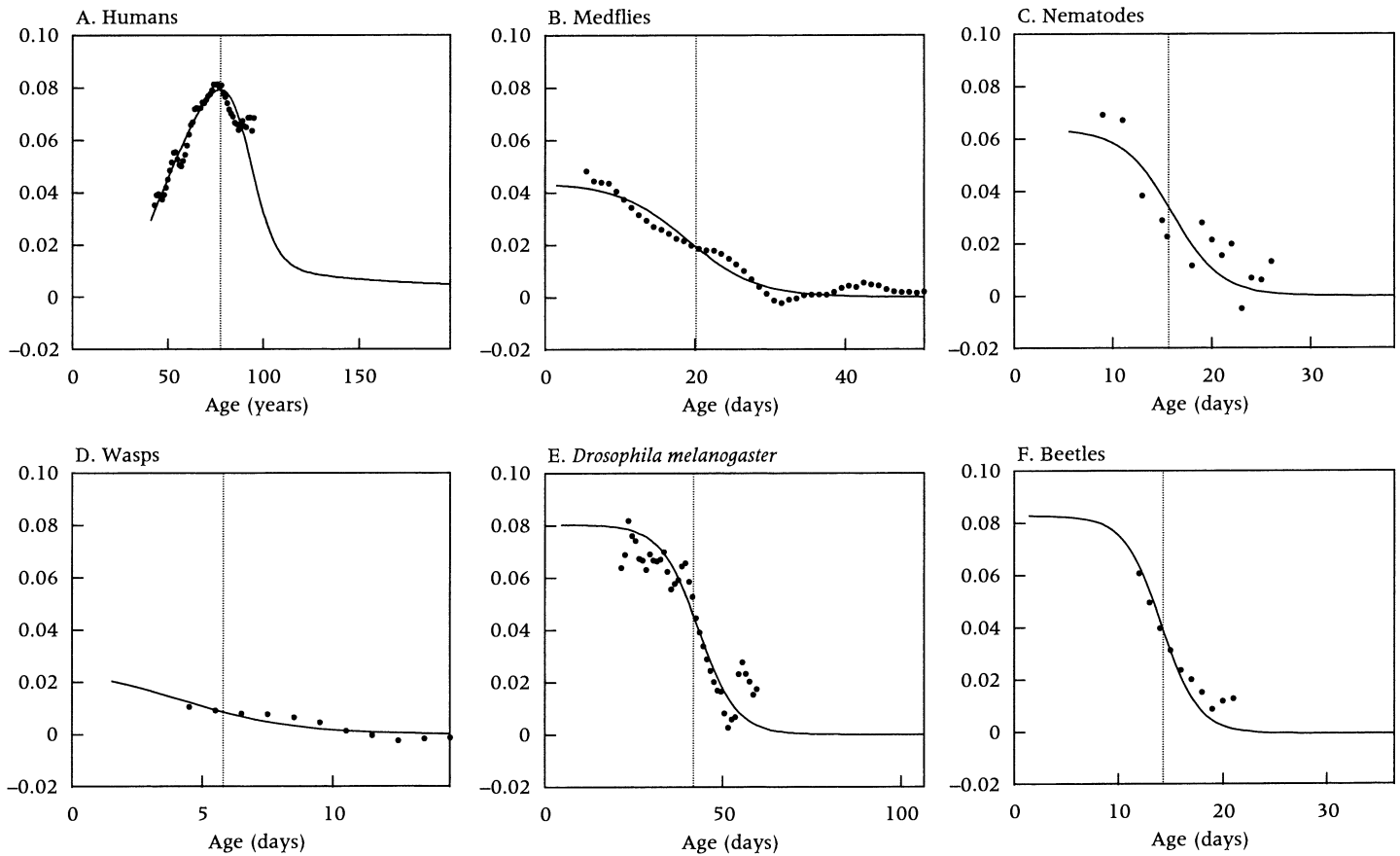

NOTE: Dots indicate values directly calculated from data, and solid lines indicate estimates using frailty models. In each panel, the vertical dotted line indicates the estimated modal life span, and the vertical axis indicates the exponential rate of mortality increase per individual-OHM. (OHM is one-hundredth of the modal life span.)
SOURCES: See Figure 1.

and 3 reveal that mortality in humans rises more steeply and slows down later than in the invertebrates.

High homogeneity of human survival: A quality control hypothesis

In invertebrates, the age-related mortality increase slows markedly around the modal age and levels off.[10] The death rate level of the plateau is in the range of 0.01 to 0.1 (per one-hundredth of the modal life span). In humans, the death rate continues to rise steeply even after having passed the death rate of 0.1 around the modal age. Thus, the life span–adjusted death rate at the modal age is considerably higher for humans than for the invertebrates (Table 1 and Figure2).[11]

A close look at the figures reveals that mortality deceleration occurs in humans after around age 75 years, as indicated by the slight concavity of the mortality curve (Figure 2A) and the short fall of the life table aging rate (Figure 3A). However, the deceleration is less pronounced and occurs with considerably higher death rates in humans than in invertebrates. The mathematical model predicts a significant slowing of human mortality after age 100 years (solid lines in Figures 2A and 3A), but the 1881–85 Swedish cohort became almost extinct around age 100.[12]

Mortality deceleration at the population level could be produced by age-related physiological and behavioral changes in individual members. It could also be due to population heterogeneity: more frail individuals tend to die at younger ages, thereby making survivors to older ages a special group of healthy individuals. This selective survival process counteracts the age-related increase of mortality risk at the individual level. If the population is more homogeneous, the mortality deceleration starts later (Horiuchi and Wilmoth 1998: Appendix A).[13]

The frailty model analysis produced estimates of the coefficient of variation, which measures the size of individual differences in vulnerability to mortality risk. Table 1 shows that the coefficient of variation for humans is the lowest, 58 percent of the coefficient of variation for nematodes (the second lowest) and 41 percent of the coefficient of variation for wasps (the highest).[14] The results shown in Table 1 and Figures 1, 2, and 3 suggest that the human cohort is more homogeneous than the invertebrate cohorts.

Because all individuals in each invertebrate cohort were reared in essentially the same environment, their life span differences may be at least partly genetic. Not surprisingly, the coefficients of variation for genetically homogeneous populations (inbred lines of nematodes and *Drosophila*) are the first and second lowest among the invertebrates. Among the other three populations, the coefficient of variation for beetles is smaller than those of medflies and wasps. The genetic diversity of the beetle co-

TABLE 1 Estimates of the coefficient of variation (CV) in vulnerability to mortality risk and estimates of the death rate per OHM at the modal age at death (DRM)

Species	CV	DRM
Humans	0.544	.0984
Mediterranean fruit flies	1.152	.0188
Nematode worms	0.942	.0337
Parasitoid wasps	1.339	.0085
Drosophila melanogaster	0.964	.0417
Bean beetles	1.138	.0363

NOTE: OHM is one-hundredth of the modal life span. See discussion in the text.
SOURCE: See Figure 1.

hort may be limited, because the 829 beetles were offspring of only 19 male–female pairs.

Large differences in the coefficient of variation between humans and two genetically heterogeneous invertebrate cohorts (medflies and wasps) suggest that genetic variations in the level of somatic maintenance may be greater in invertebrates than in humans. It is puzzling, however, that estimated individual differences in survivability are smaller in the genetically heterogeneous Swedish cohort than in the genetically homogeneous nematode and *Drosophila* cohorts.

Finch and Kirkwood (2000) argue that in addition to genes and the external environment in which individuals live after birth, "chance" is a major source of individual differences. In particular, in embryo development from fertilized ovum to birth or hatching, random events and fluctuations occur at the molecular, cellular, and other levels, affecting physiological and morphological characteristics of the organism. Considerable phenotypical variations have been found among individuals (even among fetuses) in genetically homogeneous populations of some species.

The wide dispersion of life span in the nematode and *Drosophila* cohorts indicates that chance may be an important source of individual differences in invertebrates. The narrow distribution of life span in the Swedish cohort suggests that chance variations and their effects are constrained more tightly in humans than in invertebrates. This may be explained by importing the concept of "quality control" from reliability engineering.

A large number of industrial products of the same model are manufactured in factories. The manufacturers expect most of the products to keep functioning properly for a certain duration of time or longer, unless the products are damaged by accidents, inappropriate use, or unusual circumstances (i.e., mortality risks in the external environment). A certain proportion of the products, however, may not be durable enough, because of errors (mistakes, accidents, and random fluctuations) that occurred to them

during the manufacturing processes. The purpose of quality control is to increase the proportion of final products that are satisfactorily durable. Measures taken to achieve this goal include reduction of the frequency and extent of errors, detection and correction of errors, control of adverse consequences of uncorrected errors, and identification and elimination of defective products.

It is possible to think of a biological analogue of quality control. Chance variations in embryo development and their potentially detrimental effects on somatic durability may be more tightly controlled, thereby decreasing the proportion of newborn individuals that are not capable of surviving long enough to achieve reproductive success.

It seems useful to distinguish between two types of defective embryos. First, some embryos will not be able to survive to the adult form. Many of them may suffer from errors in gametogenesis and meiosis and result in natural abortions, hatching failures, and larval deaths, without any direct effects on the distribution of adult life span. Second, some embryos are "substandard." They are viable in the adult form but their prospective fitness is considerably lower than expected from their genotypes.[15] Reduced production of these embryos and their elimination before birth or during early development could affect the distribution of adult life span if their low fitness comes from their low survival abilities.

The timing and effectiveness of quality control may be related to such factors as the cost of pregnancy, parental care, and number of offspring. It would be advantageous for defective embryos to be discarded as early as possible if the cost of pregnancy (in terms of length, energy, etc.) is high.[16] Quality control increases the cost-effectiveness of parental investment, particularly if offspring require parental care. A smaller number of offspring may make it more important to have no or few children who have "substandard" fitness.

Quality control in manufacturing shifts the peak of product life distribution to the right by reducing the number of products that are not durable enough. Without changes in the fundamental design of the product, however, the maximum length of product life remains unchanged, that is, the end of the right tail of the distribution cannot move further to the right. Therefore, quality control compresses the failure time distribution to the right and rectangularizes the product's survival curve. The variation in the product's life span is thereby reduced, and the distribution is skewed to the left. It seems reasonable to expect that quality control in embryo development should have similar effects on the life span distribution of living organisms.

In summary, the differences between humans and invertebrates in the relative timing of mortality deceleration and the shape of the life span distribution may be explained by the following "quality control" hypothesis. Chance variations in embryo development and their potentially adverse ef-

fects are more tightly controlled in humans than in invertebrates, which makes human populations more homogeneous than invertebrate populations with respect to the level of somatic maintenance.

Mortality acceleration in humans: A repair senescence hypothesis

A steeper mortality increase tends to make the life span distribution more narrowly concentrated around the peak. In humans, the death rate starts to ascend around age 40 and continues to rise steeply (Figure 2A), as implied by high values of the life table aging rate in Figure 3A.[17] The rapid age-associated increase of human mortality makes the death rate (per one-hundredth of the modal life span) at the modal age greater, the peak of life span distribution higher, and the relative life span variation smaller in humans than in invertebrates.

Figure 3 reveals, however, that the mortality increase is not necessarily faster (i.e., the life table aging rate is not necessarily greater) for humans in their 40s than for invertebrates in the corresponding age ranges (around the midpoint between age 0 and the modal age). The mortality increase around the modal age is the steepest in humans because the slope of the logarithmic mortality curve becomes progressively steeper from about age 40 to about age 75. The acceleration of mortality increase is substantial, from nearly 4 percent per one-hundredth of the modal life span (5 percent per year) around age 40 to about 8 percent per one-hundredth of the modal life span (10 percent per year) around age 75 (Figure 3A). Such a distinct phase of mortality acceleration is absent in all five invertebrate cohorts. The age-associated relative increase in mortality accelerates significantly at younger old ages in humans, but not in invertebrates.[18]

Thus, the overall life table aging rate patterns are strikingly different between humans and invertebrates. In humans, it rises first, then declines. The bell-shaped pattern, indicating a combination of mortality acceleration at younger old ages and deceleration at older old ages, has been observed widely among human populations of various countries in different periods, in both cohort and period life tables (Coale and Guo 1989; Horiuchi and Coale 1990; Horiuchi 1997; Horiuchi and Wilmoth 1998).[19] In contrast, the life table aging rate declines with age (i.e., the age-associated relative increase of mortality decelerates) fairly consistently in all of the invertebrate species.[20]

The frailty model analysis suggests that the cohort mortality acceleration reflects underlying mortality patterns of individuals. Figure 4 displays estimated mortality risks for the standard human and standard medfly.[21] The human log-mortality curve is notably convex, implying a significant acceleration of mortality risk at the individual level.[22]

FIGURE 4 Estimated age trajectory of mortality risk at the individual level, for the standard human and standard medfly

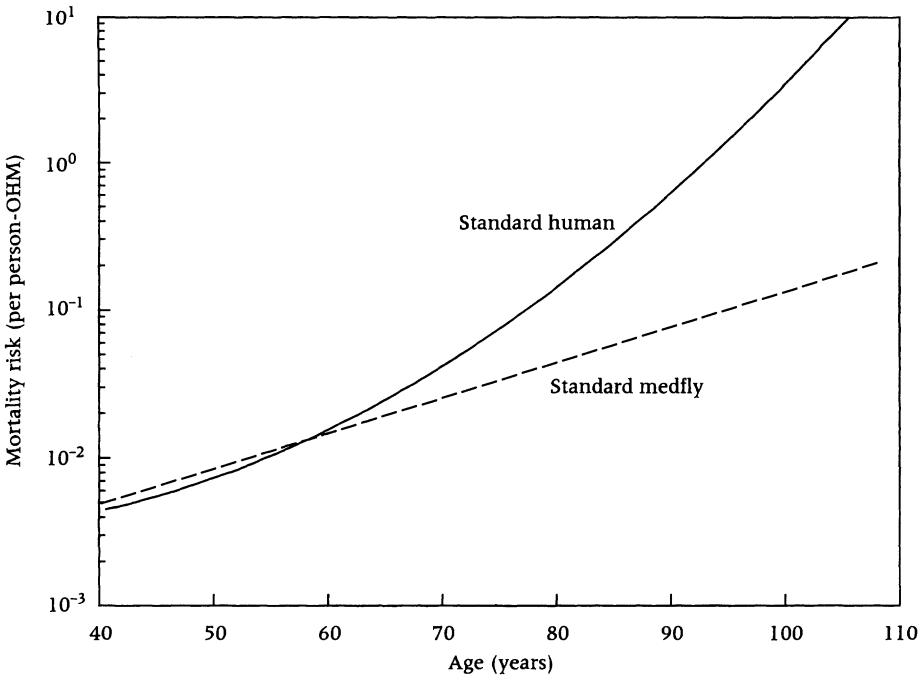

NOTE: The horizontal axis shows human age. Medfly ages were converted to corresponding human ages by equalizing the modal life spans of the two cohorts. The vertical axis indicates the number of deaths per individual-OHM of exposure. (OHM is one-hundredth of the modal life span.) In this analysis, the standard human is a person whose mortality risk at age 40.5 years is equal to the cohort average, and the standard medfly is a medfly whose mortality risk at age 1.0 day is equal to the cohort average.
SOURCES: See Figure 1.

Mortality increase may be related to damage accumulation.[23] Mechanisms of somatic maintenance are not perfect, allowing damage to accumulate (Kirkwood 1997). The mathematical model of senescence developed by Strehler and Mildvan (1960) suggests that if damage accumulates at a constant rate, the trajectory of logarithmic mortality risk is linear (Gompertzian). However, a modified version of the Strehler–Mildvan model suggests that if the mechanisms for preventing and repairing damage deteriorate with age, damage accumulates at an increasing rate and the trajectory of logarithmic mortality risk is quadratic and convex. (See Appendix B for the mathematical derivation.)

It is reasonable to assume that functions of damage prevention and repair decline with age. Various immune functions deteriorate with age (Miller 1995). The rate of protein degradation declines with age, and this is likely to allow abnormal proteins to accumulate (Van Remmen et al. 1995). Wound healing is slower at older ages (Chuttani and Gilchrest 1995). The ability to mount acute host defenses to oxidant injury decreases with age in

rats (Ikeyama et al. 2002). The apoptotic response to genotoxic stress declines with age in mice (Suh et al. 2002).

Damage prevention and repair are probably important for most species. In particular, long-lived species are expected to have highly efficient mechanisms of damage prevention and repair that can keep the organism functioning for a few decades or longer. Therefore, it seems possible that senescence in long-lived species is strongly affected by the deterioration of prevention and repair functions later in life, whereas senescence in short-lived species is mainly attributable to relatively low effectiveness of prevention and repair mechanisms, which makes the rate of damage accumulation already high early in life.

The preceding discussion can be summarized as follows. In long-lived species, highly effective mechanisms of damage prevention and repair make their senescent processes slower than in short-lived species. However, the age-related deterioration of prevention and repair mechanisms may make the senescent processes of long-lived species more accelerated than those of short-lived species. This "repair senescence" hypothesis is consistent with the accelerated relative increase of the human death rate at younger old ages.[24]

Conclusions

This study compared variations and differences in life table functions relative to the modal life span. Relative and absolute variations should be distinguished strictly and carefully.

In addition, the interspecies comparison has at least three major limitations. First, because of data availability, comparison was made between two extremes: humans versus invertebrates. It would be desirable to include, for example, some mammalian species that live for a few to several years. To study shapes of life table functions, however, requires a large number of observations that produces fairly smooth age trajectories up to very old ages. Although many studies have been conducted on mice and rats, rodent survival data on cohorts that are sufficiently large for analysis of life table aging rates, to the knowledge of this author, do not exist. (Appendix D shows survival data on 223 mice and 205 dogs just for crude comparison with humans and invertebrates, but the method of analysis and reliability of the results are very limited because of the small cohort sizes.)

Second, animal populations, after being exposed to the force of gene selection (or the lack of it) in the laboratory for many generations, may differ significantly in the size of genetic variations from their ancestors in the natural world. This applies to modern humans as well. Life table patterns in protected populations may not sensitively reflect the effects of natural selection on the abilities of somatic maintenance in the wild.

Third, although both humans in modern societies and animals in laboratories can be considered to live in protected environments, their conditions may not be highly comparable. The laboratory animals were more strictly protected from epidemics and food shortage and probably from violence than were Europeans born in the late nineteenth century.[25] On the other hand, contemporary humans (and, to a lesser extent, pet animals) benefit greatly from modern medical care, while insects and worms in laboratories do so much less, if at all.

These limitations strongly suggest that the results of this study should be interpreted with caution. Nevertheless, the major differences between human and invertebrate life table patterns are clear enough to make us think that they may reflect some important underlying factors. Interspecies differences in the life span distribution are worthy of further investigation.

Appendix A: Data and measurement

The human data (the male Swedish cohort born in 1881–85) were downloaded from the Berkeley Mortality Database (http://www.demog. berkeley.edu/wilmoth/mortality/), which later evolved to the Human Mortality Database (http://www.mortality.org). The medfly and beetle data were drawn from Carey et al. (1995: Appendix) and Tatar and Carey (1994: Table 1), respectively, and data on the other species were provided by the authors of Vaupel et al. (1998). See these references and Johnson et al. (2001) for more information on the data.

Males and females may exhibit different mortality patterns. In this study, male data were used, except for the hermaphrodite nematodes, mainly because male medflies were preferred to female medflies. In the original study (Carey et al. 1992), the male and female medflies were maintained on a sugar-only (protein-deprived) diet. Protein deprivation alters female mortality patterns markedly but affects male patterns only mildly (Müller et al. 1997). Physiologically, female medfly mortality is more sensitive than male medfly mortality to environmental variations (Carey et al. 2001). The extent to which these sex differentials hold for other invertebrate species remains to be investigated.

The Swedish 1881–85 cohort was selected for several reasons. First, selective survival processes can be followed only in cohort mortality, and cohort data were used for the other species. Second, a cohort born more than 110 years ago was preferred, to ensure that virtually all of its members had died. Third, Sweden is one of the few countries whose demographic data during the nineteenth century were considered already highly accurate. Finally, a previous study has shown that this particular cohort followed the typical pattern of old-age mortality that was widely observed in human male and female populations (Horiuchi and Wilmoth 1998).

The life span distribution was obtained over the entire age range (except the hatching day) for medflies, wasps, and beetles, and for ages 14 years and older for humans, 4 days and older for *Drosophila*, and 5 days and older for nematodes. The death rate declined with age for the first 13 years in humans and for the first 3 days in *Drosophila*. These periods were not included in the data analysis because

the focus of this study was on longevity and senescence, not on development. Nematode mortality data during the first 4 days were not collected in the original study. The age ranges for which the life span distribution was computed can be considered to approximately represent "adult life," including both reproductive and postreproductive stages, but excluding early stages in which the death rate declines with age.

For five out of the six cohorts, deaths of all cohort members were recorded; for nematodes, samples were drawn repeatedly for measuring mortality at different ages. The nematode data set comprises results of five studies that used the same wild-type (i.e., not mutant) inbred line, TJ1060 (Johnson et al. 2001). Because dead nematodes cannot be identified immediately, it takes considerably more time to count them than dead beetles, flies, or wasps. Therefore, in each of the studies, samples were drawn every other day, and death rates for the samples during the following 24-hour period were obtained. After the cohort size had become relatively small, the entire cohort was followed.

Because of this procedure, nematode mortality data were not obtained for the 6th, 8th, 10th, 12th, 14th, and 16th days. Without death rates for these dates, it is impossible to estimate the life span distribution for the 5th day and later. Thus death rates for these dates were geometrically interpolated from death rates for the adjacent days. These interpolated death rates are neither included in Figure 2C nor used for computing life table aging rates in Figure 3C, but are used for deriving the life span distribution in Figure 1C (dots).

Because the invertebrates experience metamorphosis, their life span in this study was defined to be the length of life in the adult form. Larval survival data were not collected for those cohorts.

Ages of the invertebrate animals were counted as follows. Let "hatching day" be the day of emergence into the adult form. When an entire invertebrate cohort is followed, usually a hatching day is set up and newborn individuals are counted at the end of the day. Deaths between hatching and day's end are not counted. Ages of the cohort members were counted assuming that they were 0.5 days old at the end of the hatching day.

Four life table functions were obtained for each of the cohorts: the proportion surviving (not shown), life span distribution, age-specific death rate, and life table aging rate. Following the convention, they are denoted by $l(x)$, $d(x)$, $m(x)$, and $k(x)$. Their relationships, assuming the continuity and differentiability of these functions with respect to age x, are given by: $d(x) = -dl(x)/dx$, $m(x) = d(x)/l(x)$, and $k(x) = dm(x)/m(x)dx$.

The $d(x)$ function was scaled such that its total over the adult age range (described earlier in this appendix) is unity. For medflies, wasps, *Drosophila*, and beetles, the death rate for the age range $[x,x+1)$ was calculated by $-log(N(x+1)/N(x))$, where $N(x)$ is the number of survivors at age x. The life table aging rate at age x was obtained as the weighted least squares estimate of the slope parameter of the Gompertz model, by fitting the Gompertz equation to logarithmic death rates for an age interval centered at x.

Appendix B: Gamma Gompertz model and gamma log-quadratic model

Assumptions and estimation

In this study, frailty models were used for summarizing and interpreting the observed survival patterns. In frailty models, the mortality risk of each individual is assumed to be the product of two terms: (1) a hypothetical variable called frailty, denoted by z, and (2) a function of age x, denoted by $\mu_s(x)$ (Vaupel et al. 1979):

$$\mu(z,x) = z\mu_s(x). \tag{B.1}$$

Frailty z may be considered as the combined age-adjusted effects of genetic and environmental characteristics of the individual on his/her mortality risk, and $\mu_s(x)$ represents the combined effects of age-related physiological and behavioral changes on the mortality risk. $\mu_s(x)$ is called the "standard" mortality schedule, because it is the trajectory of mortality risk for individuals with $z = 1$, which is the mean value of z at the lowest end of the age range in which mortality is assumed to follow the model.

As in many previous studies, z is assumed to be gamma-distributed. One of the two parameters of the gamma distribution uniquely determines the coefficient of variation of z. Because of selective survival, the mean and variance of z change with age. However, z remains gamma-distributed and the coefficient of variation is constant over age (Vaupel et al. 1979).

The most widely used form for $\mu_s(x)$ is the exponential equation (Gompertz model):

$$\mu_s(x) = \mu_0 \exp(\theta x). \tag{B.2}$$

The combination of the gamma-distributed frailty in the cohort and the Gompertzian mortality risk at the individual level is called the gamma Gompertz model. The combination of the two assumptions makes the cohort death rate at age x, denoted by $m(x)$, a three-parameter logistic function of age (Beard 1959):

$$m(x) = \frac{Be^{\theta x}}{1 + Ce^{\theta x}}. \tag{B.3}$$

For the five invertebrate cohorts, the gamma Gompertz model fits $d(x)$, $m(x)$, and $k(x)$ patterns well (Figures 1, 2, and 3). The model is fundamentally incompatible with the typical old-age pattern of human mortality, however. It is mathematically impossible for the gamma Gompertz model to produce a bell-shaped $k(x)$ curve, because equation B.3 implies that $k(x)$ changes monotonically with age. Thus a modified model was adopted for humans, assuming that the age trajectory of mortality risk at the individual level follows the form:

$$\mu_s(x) = \exp(ax^2 + bx + c). \tag{B.4}$$

This pattern can be called "log-quadratic," because the logarithm of the mortality risk is a quadratic function of age. (The Gompertz equation is log-linear.) By com-

bining this equation with the gamma-distributed z, the cohort death rate at age x is given by

$$m(x) = \bar{z}(x)\exp(ax^2 + bx + c), \tag{B.5}$$

where the mean of z at age x is given by

$$\bar{z}(x) = \frac{1}{1 + \frac{1}{\alpha}\int_{x_0}^{x} \exp(at^2 + bt + c)dt}.$$

x_0 is the age at which the mortality risk starts to follow the quadratic equation, and α is the inverse of the squared coefficient of variation of the gamma distribution. The mean of z at age x_0 is one. Equation (B.5) is called the gamma log-quadratic model.

The gamma Gompertz model and the gamma log-quadratic model were fitted to age-specific death rates by the method of weighted least squares. The parameters were estimated by minimizing

$$L = \sum_i D_i(\ln M_i - \ln m_i)^2, \tag{B.6}$$

where D_i and M_i are the number of deaths and the death rate, respectively, for the i-th age group; m_i is calculated by equation B.3 or B.5. The weight, D_i, is approximately equal to the inverse of the variance of $\ln M_i$.

The *d(x)*-based method of maximum likelihood estimation (Pletcher 1999; Promislow et al. 1999) was not used, partly because it cannot be applied to the sample-based data on nematode mortality, and partly because the *m(x)*-based method seemed more sensitive to *k(x)* variations. Estimates by weighted least squares are approximately maximum likelihood estimates if, for each age group, the number of living individuals and the number of deaths are large and the death rate is not extremely high.

In model estimation, some consecutive youngest ages and/or oldest ages were excluded in order to avoid ages with fewer than ten deaths. In humans, the model was fitted to ages 40 and older because the death rate follows a smooth upward trajectory only after age 40 (i.e., $x_0 = 40.5$).

Gerontological interpretation

Equation B.4 is consistent with the idea that mechanisms for preventing and repairing somatic damage deteriorate with age. This can be shown using the model by Strehler and Mildvan (1960), in which the "vitality" of a living organism is assumed to decline linearly with age. This assumption is supported by empirical evidence that various physiological indicators change with age approximately linearly. The linear decrease of vitality is expressed as:

$$v(x) = v_0 - gx, \tag{B.7}$$

where v_0 is the initial vitality level and g is the rate of physiological decline. For simplicity, vitality is assumed to decline from age 0. If physiological conditions deteriorate with age because of accumulation of damage, g can be interpreted as the rate of damage accumulation. Strehler and Mildvan derived the Gompertz equation from the assumption of linear vitality decline.

Living organisms have mechanisms for preventing and repairing the damage. (Hereafter, only "repair" will be mentioned for simplicity; "prevention" can be treated mathematically in the same way.) Thus, the model may be modified as

$$v(x) = v_0 - (g - r)x, \tag{B.8}$$

where r is the repair rate and $0 < r < g$. However, the repair mechanisms may deteriorate with age. A simple model of this process is a linear decline of repair rate with age:

$$r(x) = r_0 - ax, \tag{B.9}$$

where r_0 is the initial repair rate and a is the rate of deterioration of repair mechanisms.

Substituting B.9 into B.8 and using the vitality–mortality relationship in the Strehler–Mildvan model, we get:

$$\mu(x) = \exp(ax^2 + bx + c),$$

where $b = g - r_0 > 0$ and $c = -v_0 < 0$. (If this process does not start at age 0 but at a certain age x_0, then $b = g - r_0 - 2ax_0$ and $c = -v_0 - gx_0 + r_0x_0 + ax_0^2$.)

The log-quadratic equation is consistent with results of three previous studies on human mortality. First, in a study on longevity of Danish twins, the underlying pattern of mortality risk of individuals was estimated, using a semi-parametric frailty model. The derived mortality trajectory was noticeably log-convex (Yashin and Iachine 1997). Second, a multivariate hazard model analysis was applied to genealogical records on British noblemen. The estimated age pattern of mortality beyond age 50 years at the individual level was also log-convex (Doblhammer and Oeppen 2002).

Third, it has been shown that major medical causes of death have significantly different age trajectories of mortality at younger old ages. The age pattern is associated with the selectiveness of the cause. Diseases with well-known strong effects of risk factors (such as cancers, liver cirrhosis, and hemorrhagic stroke) can be considered highly selective, because individuals who have the risk factors are particularly vulnerable. Mortality curves of those diseases tend to be log-concave, and patterns of diseases that are considered less selective (such as pneumonia, gastroenteritis, and congestive heart failure) tend to be log-convex (Horiuchi and Wilmoth 1997, 1998). Greater selectivity, whether it is due to environmental or genetic differences, makes the mortality curve more log-concave. Therefore, the differential trajectories of cause-specific mortality suggest that age patterns of total mortality risk of individuals, which are not distorted by selection, might be even more log-convex than those of aggregate-level death rates from less selective diseases.

Appendix C: Simulation of relationships between mortality pattern and life span distribution

A simulation study was conducted to investigate relationships between the age pattern of mortality and the shape of life span distribution. The three-parameter logistic equation (gamma Gompertz model), which was fitted to death rates for the five invertebrate cohorts (but not those for the human cohort), was used for generating hypothetical mortality schedules.

For this simulation, the widely used form (equation B.3) was converted into:

$$m(x) = \frac{\lambda e^{\theta x}}{1 + \frac{\lambda}{\alpha\theta}(e^{\theta x} - 1)}, \tag{C.1}$$

because the parameters in this form can be more easily interpreted than those in equation B.3 (Vaupel 1990). λ is the death rate at age zero (i.e., $\lambda = m(0)$), θ affects the steepness of age-related mortality increase, and α is negatively associated with the timing of mortality deceleration. By combining different values of these parameters, 150 life tables were produced. In all of the life tables, the modal life span was fixed at 100 years. The ranges of λ, θ, and α are [0.00002, 0.00230], [0.0202, 0.0838], and [0.444, 3.400]. These ranges cover λ, θ, and α values estimated for the five invertebrate cohorts as well as α for the Swedish cohort. (Note that α values in the gamma Gompertz and gamma log-quadratic models are comparable.)

Relationships between these three parameters and two measures of life span distribution were examined. The two variables are (1) the density at the modal age (i.e., the height of the peak), which measures the dispersion/concentration of deaths around the modal age, and (2) the proportion of all deaths between ages 0 and 200 that occur under age 100, which indicates the extent of skewness to the left.

Major results of the simulation are shown in Figure 5. Panel A shows that if the modal life span is fixed, λ and θ are negatively associated. That is, the same modal life span could be derived from a combination of low initial mortality and steep mortality rise and a combination of high initial mortality and slow mortality rise. (Note that although θ is not a life table aging rate, θ and the life table aging rate are on the same scale. Thus, the horizontal axes of the three panels of Figure 5 are directly comparable to the vertical axes of Figure 3. In particular, if α is infinitely large, equation C.1 becomes the Gompertz model, in which θ is the age-independent life table aging rate.)

Because of the strong correlation between λ and θ, the other two panels of Figure 5 use θ, but not λ. Panel B indicates that both a steeper rise of mortality (necessarily combined with lower initial mortality) and a later start of mortality deceleration make the life span variation smaller and the peak of distribution higher. Note that the vertical axis of this panel is directly comparable to the vertical axes of Figure 1.

Panel C reveals that greater delay of mortality deceleration skews the life span distribution more to the left. The life span distribution is exactly symmetric if α is unity (i.e., if frailty is exponentially distributed). The effect of steepness of mortal-

FIGURE 5 Simulated relationships between mortality pattern and life span distribution

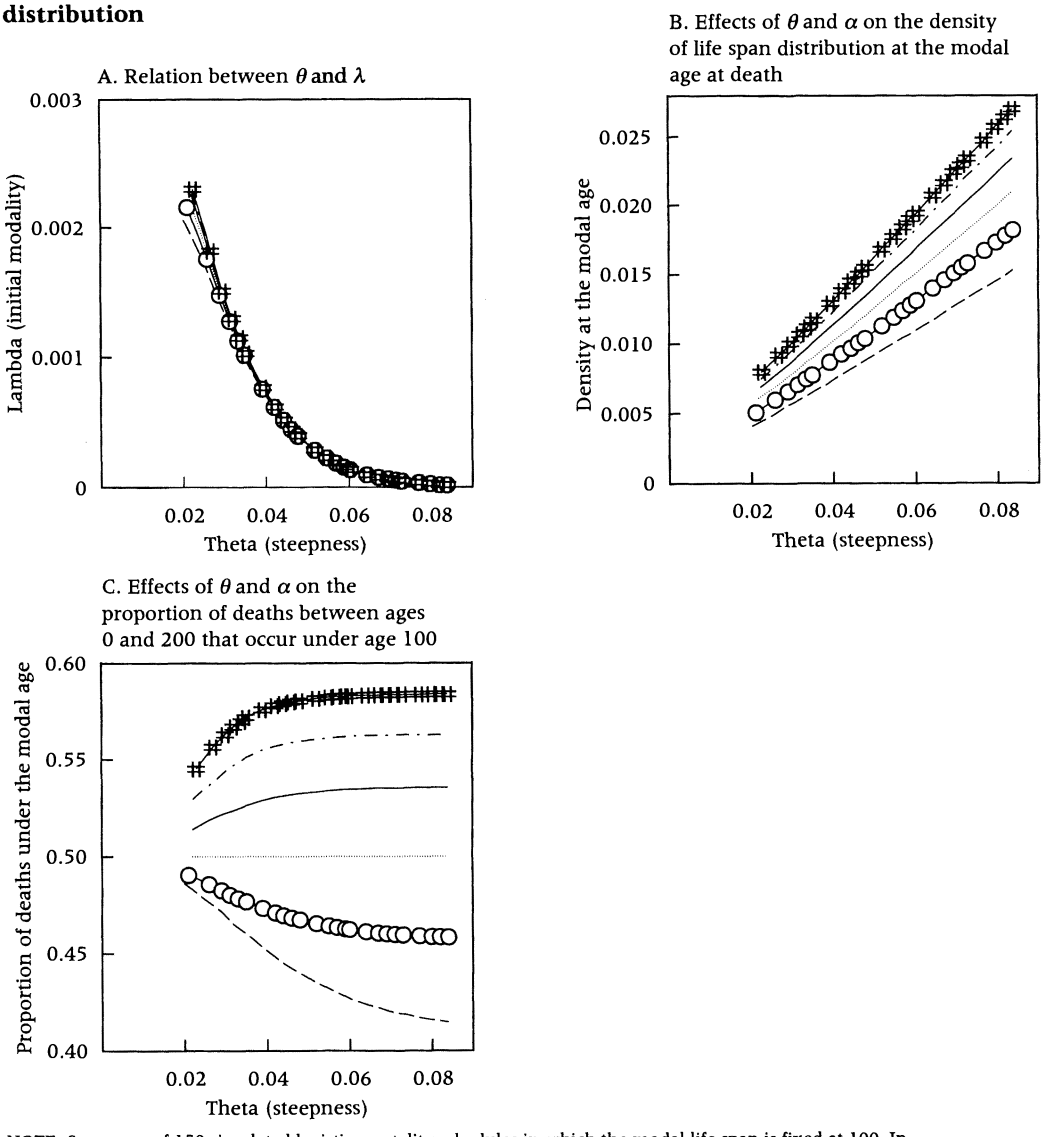

NOTE: Summary of 150 simulated logistic mortality schedules in which the modal life span is fixed at 100. In the majority of the mortality schedules, almost 100 percent of deaths occur under age 200. In all three panels, the six curves indicate different α values: 4/9 (dashed), 2/3 (circle), 1 (dotted), 1.5 (solid), 2.25 (dash-dot) and 3.4 (asterisk). For definitions of λ, θ, and α, see equation C.1.

ity rise on the skewness depends on the timing of mortality deceleration, and does not appear substantial for left-skewed distributions, as indicated by the upper three curves. Although these results are based on the particular mathematical model, it seems reasonable to expect the same directions of relationship for typical patterns of adult mortality in empirical life tables.

Appendix D: Life span distribution in mice and dogs

Figure 6 displays life span distributions and mortality patterns for an inbred line ($B6CF_1$) of 223 mice and a cohort of 205 beagle dogs. The data have been drawn from a previous study of interspecies mortality comparison (Carnes, Olshansky, and Grahn 1996). Figure 6 was produced in the same way as Figures 1 and 2. The solid lines indicate the gamma Gompertz model fitted to the data. The estimated modal life span, indicated by the vertical dotted line, is 952 days for mice and 4,704 days for beagle dogs. Because of the small size of each cohort, it is impossible to obtain a smooth sequence of reliable life table aging rates. Thus, we cannot examine whether the relative mortality increase with age accelerates at younger old ages in these cohorts.

FIGURE 6 Life span distribution (A and B) and age-specific death rates (C and D) for mice and dogs

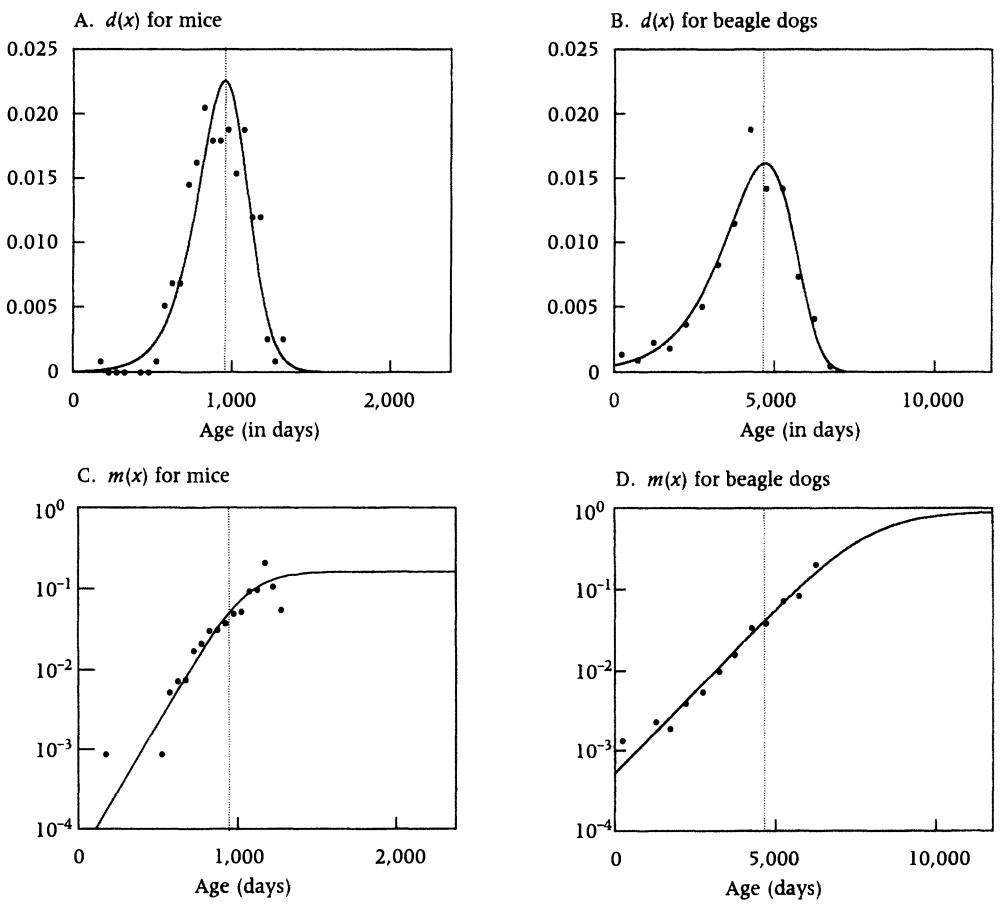

NOTE: Produced in the same way as Figures 1 and 2.
SOURCE: Carnes, Olshansky, and Grahn 1996.

The skewness of the life span distribution splits vertebrates and invertebrates clearly. The three mammalian curves are more skewed than the five invertebrate curves. Thus, estimated coefficients of variation for mice and dogs (0.680 and 0.221) are smaller than those for invertebrates. Moreover, their coefficients of variation are closer to the human figure (0.544) than to the figure for the lowest invertebrate (0.942). If we expect quality control in embryogenesis to be tighter among vertebrates than invertebrates, this result is consistent with the conjecture.

It appears puzzling that in terms of the estimated coefficient of variation, humans are placed between mice and dogs. However, it is possible that dogs of the same breed living in the same laboratory are far more homogeneous in mortality risk than people in an entire country. In addition, the very low coefficient of variation of the dogs may simply be a statistical artifact of the cohort size, which might have become too small before the starting age of noticeable mortality deceleration.

The height of the peak of the life span distribution fails to distinguish vertebrates and invertebrates clearly. Although the estimated peak for mice is the second highest, the peak for dogs is lower than peaks for *Drosophila* and beetles. This seems due to the slope of the mortality curve for dogs before the modal age, which is apparently less steep than the slopes for *Drosophila* and beetles. Therefore, of the two major features of human life span distribution in Figure 1A, the great skewness may be more biologically essential than the high peak.

Because of the small cohort sizes, however, these results should not be taken as highly reliable. For this type of analysis, it is desirable to collect survival data for considerably larger mammalian cohorts.

Notes

I thank James Carey, James Curtsinger, Thomas Johnson, S. Jay Olshansky, Vladimir Shkolnikov, and James Vaupel for providing data. I am also grateful to Caleb Finch, Thomas Johnson, Ryuichi Kaneko, S. Jay Olshansky, and James Vaupel for useful comments on earlier versions. This research was supported by grants K02-AG00778 and R01-AG14698 from the US National Institute on Aging, National Institutes of Health.

1 However, a higher proportion of human deaths at younger adult ages than at older ages is due to injuries (including accidents, suicide, and homicide) and infectious diseases (see, for example, Horiuchi 1999: Figure 2). Probably this is why both the proportion of the life span and the death rate for the Swedish cohort rise smoothly and consistently after age 40 years, but not under age 40 (Figures 1A and 2A).

2 These two effects cannot be separated in a mechanistic manner. In order to investigate these two effects on the life span distribution, additional information and/or assumptions are needed.

3 The exact size of the nematode cohort is not known, because samples were drawn from the cohort.

4 A very small proportion of the nematodes were males. They were not included in the mortality measurement.

5 The modal life span is 79.5 years for humans, 20.2 days for medflies, 15.7 days for nematodes, 5.8 days for wasps, 42.8 days for *Drosophila*, and 14.7 days for beetles. Because the life span distribution was erratic in some of the cohorts, modal ages estimated by mathematical models were adopted.

6 Although the modal life span is not used as widely as the mean life span (life expectancy) and median life span, the usefulness of the modal life span in aging research has been increasingly recognized (e.g., Kannisto 2001).

7 For example, neonatal deaths can be distinguished from perinatal miscarriages and stillbirths fairly accurately in humans and large-sized mammalian species. This distinction is a necessary condition for measuring infant mortality and life expectancy at birth in human demography. Usually the distinction is difficult or meaningless, however, when invertebrate eggs hatch and go through metamorphosis.

8 The vertical axes of Figures 1, 2, and 3 are the proportion of deaths per one-hundredth of the modal life span (OHM), the number of deaths per individual-OHM, and the exponential rate of mortality increase per OHM, respectively. These OHM-based life table functions can be obtained simply by calculating them in terms of the conventional time unit (year or day), multiplying them by the modal life span (in the same conventional time unit), and dividing by 100.

9 In this context, "being skewed to the left" means that the left arm of the bell-shaped curve is less steep than the right arm.

10 Although some old-age death rates in Figure 2 (in particular, those for nematodes, *Drosophila*, and beetles) appear to be far above the estimated plateau, most of those points are based on small numbers of deaths and have large stochastic variations. In medflies and wasps, the death rate not only reaches a plateau, but decreases noticeably at very old ages (Vaupel et al. 1998). This occurs outside the age range of Figure 2B. The three-parameter logistic model cannot capture this part of the mortality trajectory.

11 Also note that the death rate and the life table aging rate are exactly equal at the modal age, which is a mathematical characteristic of the life table.

12 An international data set that includes a relatively large number of centenarians and super-centenarians (ages above 110 years) has revealed that the mortality increase slows down considerably after age 100 (Kannisto 1994; Thatcher, Kannisto, and Vaupel 1998). This finding is consistent with the extrapolated mortality deceleration in Figures 2A and 3A.

13 The heterogeneity hypothesis explains not only the occurrence of mortality deceleration but also various related phenomena (reviewed in Wilmoth and Horiuchi 1999; also Ewbank 2001). A major issue raised about the heterogeneity hypothesis is that individual differences estimated by frailty models tend to greatly exceed variations of quantitative physiological traits that are usually observed among individuals of the same species. It is important, however, to strictly distinguish between physiological variations and risk variations. Small physiological differences may lead to large differences in mortality risk.

At least two kinds of data suggest substantial individual variations in mortality risk. First, age variations in mortality are considerably larger than age variations in physiological characteristics. In the Swedish male cohort born in 1881–85, the death rate increased by more than ten times from age 40 to age 73. It seems difficult, on the other hand, to find quantitative physiological traits with tenfold differences between 40-year-old and 73-year-old persons. Second, many epidemiological studies indicate substantial individual differences in mortality risk. According to a multivariate hazard model analysis of data from National Health Interview Surveys in the United States, the mortality risk (adjusted for age and income) in 1990–95 for "divorced/separated and unemployed black males with less than 12 years of education" is 9.38 times higher (= 1.36 x 1.78 x 1.25 x 2.00 x 1.55) than for "married and employed non-black females with 16 or more years of education" (Rogers, Hummer, and Nam 2000: Table 3.2). These two are the highest and lowest risk profiles that have been produced by only five basic demographic and socioeconomic factors (sex, race, education, marital status, and employment status). This risk difference corresponds to the 94.5 percent median-centered range (97.25 percentile versus 2.75 percentile) in the frailty distribution estimated for the Swedish cohort and to the 57.0 percent range for the medfly cohort. Additional inclusion of four health-behavior factors (smoking, alcohol consumption, exercise, and obesity) increases the ratio further to 32.85, corresponding to the 99.6 percent range for the Swedish cohort and to the 76.9 percent range for medflies (ibid.: Table 3.3). Thus, individual differences estimated by frailty model analyses do not seem far greater than those estimated from epidemiological data.

14 This is not a statistical artifact of using different models (the gamma log-quadratic

model for humans and the gamma Gompertz model for the others), because the latter model produced a lower estimate of the coefficient of variation for humans than the former model.

15 Gavrilov and Gavrilova (2001) have developed reliability-theoretical models of mortality and senescence, in which living organisms are assumed to be born with stochastically varying numbers of nonfatal defects.

16 It is believed that a high proportion of human embryos are aborted before diagnosis of the pregnancies and even before implantation of the fertilized eggs, though it has not been feasible to estimate the proportion involved (Ellison 2001: chapter 2).

17 The life table aging rate (LAR) is the rate of relative mortality increase with age. A rise of LAR indicates an acceleration of age-related proportional increase in mortality (a convex curvature of the logarithmic mortality curve); a decline of LAR indicates a deceleration (a concave curvature); and a constant LAR implies an exponential mortality increase (a straight line). Figure 3 reveals that with respect to the assumed constancy of the life table aging rate, all of the cohorts deviate considerably from the Gompertz model. The striking difference between human and invertebrate patterns suggests that the life table aging rate is a powerful statistical tool for biodemography. Detailed descriptions of the rate are given in Horiuchi and Wilmoth (1997, 1998).

18 It is necessary to distinguish relative (proportional, geometric) and absolute increases. In humans, the absolute mortality increase usually continues to accelerate throughout adult ages up to around 100 years or more, but the relative mortality increase starts to slow down around age 75.

19 Male populations in some industrialized countries deviate from this typical bell-shaped pattern of the life table aging rate (Horiuchi 1997). The deviation may be related to the diffusion of smoking after World War I. Historical time series of mortality data for Sweden have revealed that male mortality in the nineteenth century followed the bell-shaped pattern, but the deviation emerged and became noticeable during the twentieth century (Horiuchi and Wilmoth 1998). My analysis of the time series of cause-specific mortality in France since 1925 has shown that smoking-related diseases such as lung cancer contributed significantly to the deviation (unpublished results).

20 The difference between humans and invertebrates can be seen, though less clearly, in curvatures of death rate functions as well (Figure 2). The logarithmic mortality curves for invertebrates appear consistently concave, as implied by the declines in the life table aging rate. However, the logarithmic mortality curve for humans is convex from around age 40 to around age 76, and concave thereafter. It may not be easy to visually detect these curvatures in the death rate function, but life table aging rates in Figure 3A show clearly that the accelerations and decelerations are significant.

21 The standard individual is a person whose mortality risk at a given age is equal to the cohort average. In this analysis, age 40.5 years for humans and age 1.0 day for medflies were used as the reference ages. These are the ages at which death rates of the respective cohorts are assumed to follow the adopted mathematical models.

22 The model estimates that the mortality risk at the individual level continues to accelerate, but the mortality rate at the aggregate level ceases to accelerate and starts to decelerate around age 76 years. The divergence between these two levels occurs at older old ages because the effect of selective survival on the age pattern of mortality is stronger at ages characterized by a higher death rate.

23 In particular, accumulation of DNA damage seems to play an essential role in senescence (de Boer et al. 2002; Stern et al. 2002).

24 The human mortality acceleration at younger old ages contributed to the reduction of life span variation. In general, however, a high concentration of deaths around the modal age does not necessarily imply a mortality acceleration. More essential for death concentration is a high level of mortality around the modal age, which could be reached not only by an accelerated mortality increase but also by a steep constant increase.

25 Deaths from accidents, suicide, homicide, and infectious diseases at younger adult ages might have contributed to the asymmetry of life span distribution for the Swedish cohort.

References

Beard, R. E. 1959. "Note on some mathematical mortality models," in G. E. W. Wolstenholme and M. O'Connor (eds.), *CIBA Foundation Colloquia on Ageing, The Life Span of Animals 5*. Boston: Little, Brown and Company, pp. 302–311.

Carey, James R. and Debra S. Judge. 2000. *Longevity Records: Life Spans of Mammals, Birds, Amphibians, Reptiles and Fish*. Odense: Odense University Press.

Carey, J. R., P. Liedo, H. G. Müller, J. L. Wang, B. Love, L. Harshman, and L. Partridge. 2001. "Female sensitivity to diet and irradiation treatments underlies sex-mortality differentials in the Mediterranean fruit fly," *Journal of Gerontology: Biological Sciences* 56(2): B89–93.

Carey, J. R., P. Leido, D. Orozco, M. Tatar, and J. W. Vaupel. 1995. "A male-female longevity paradox in medfly cohorts," *Journal of Animal Ecology* 64: 107–116.

Carey, J. R., P. Liedo, D. Orozco, and J. W. Vaupel. 1992. "Slowing of mortality rates at older ages in large medfly cohorts," *Science* 258: 458–461.

Carnes, B. A., S. J. Olshansky, and D. Grahn. 1996. "Continuing the search for a fundamental law of mortality," *Population and Development Review* 22: 231–264.

Chuttani, A. and B. A. Gilchrest. 1995. "Chapter 11. Skin," in Edward J. Masoro (ed.), *Handbook of Physiology: Section 11: Aging*. New York: Oxford University Press, pp. 309–324.

Coale, A. J. and G. Guo. 1989. "Revised regional model life tables at very low levels of mortality," *Population Index* 55: 613–643.

Comfort, A. 1979. *The Biology of Senescence*. New York: Elsevier.

de Boer, Jan, Jaan Olle Andressoo, Jan de Wit, Jan Huijmans, Rudolph B. Beems, Harry van Steeg, Geert Weeda, Gijsbertus T. J. van der Horst, Wibeke van Leeuwen, Axel P. N. Themmen, Morteza Meradji, and Jan H. J. Hoeijmakers. 2002. "Premature aging in mice deficient in DNA repair and transcription," *Science* 296: 1276–1279.

Doblhammer, Gabriele and Jim Oeppen. 2002. "Reproduction and longevity among the British peerage: The effect of frailty and health selection," unpublished paper presented at the annual meeting of the Population Association of America, 9–11 May, Atlanta.

Ellison, Peter T. 2001. *On Fertile Ground: A Natural History of Human Reproduction*. Cambridge: Harvard University Press.

Ewbank, Douglas C. 2001. "Demography in the age of genomics: A first look at the prospects," in C. E. Finch, J. W. Vaupel and K. Kinsella (eds.), *Cells and Surveys*. Washington, DC: National Academy Press.

Finch, Caleb E. 1990. *Longevity, Senescence, and the Genome*. Chicago: The University of Chicago Press.

Finch, Caleb E. and Thomas B. L. Kirkwood. 2000. *Chance, Development, and Aging*. New York: Oxford University Press.

Finch, C. E. and M. C. Pike. 1996. "Maximum life span predictions from the Gompertz mortality model," *Journal of Gerontology: Biological Sciences* 51(3): B183–B194.

Gavrilov, Leonid A. and Natalia S. Gavrilova. 2001. "The reliability theory of aging and longevity," *Journal of Theoretical Biology* 213: 527–545

Horiuchi, S. 1997. "Postmenopausal acceleration of age-related mortality increase," *Journal of Gerontology: Biological Sciences* 52(1): B78–92.

Horiuchi, S. 1999. "Epidemiological transitions in human history," in *Health and Mortality: Issues of Global Concern*. New York: United Nations, pp. 54–71.

Horiuchi, S. and A. J. Coale. 1990. "Age patterns of mortality for older women: An analysis using the age-specific rate of mortality change with age," *Mathematical Population Studies* 2: 245–267.

Horiuchi, S. and J. R. Wilmoth. 1997. "Age patterns of the life-table aging rate for major causes of death in Japan, 1951–1990," *Journal of Gerontology: Biological Sciences* 52A: B67–B77.

Horiuchi, S. and J. R. Wilmoth. 1998. "Deceleration in the age pattern of mortality at older ages," *Demography* 35(4): 391–412.

Ikeyama, S., G. Kokkonen, S. Shack, and X. T. Wang. 2002. "Loss in oxidative stress tolerance with aging linked to reduced extracellular signal-regulated kinase and Akt kinase activities," *FASEB Journal* 16(1): 114–116.

Johnson, Thomas E., Deqing Wu, Patricia Tedesco, Shale Dames, and James W. Vaupel. 2001. "Age-specific demographic profiles of longevity mutants in *Caenorhabditis elegans* show segmental effects," *Journal of Gerontology: Biological Sciences* 56: B331–B339.

Kannisto, V. 1994. *Development of Oldest-Old Mortality, 1950–1990: Evidence from 28 Developed Countries*. Odense: Odense University Press.

Kannisto, V. 2001. "Mode and dispersion of the length of life," *Population: An English Selection* 13(1): 159–172.

Kirkwood, T. B. 1997. "The origins of human ageing," *Philosophical Transactions of the Royal Society of London—Series B: Biological Sciences* 352(1363): 1765–1772.

Miller, Richard A. 1995. "Immune system," in Edward J. Masoro (ed.), *Handbook of Physiology: Section 11: Aging*. New York: Oxford University Press, pp. 555–590.

Müller, H. G., J. L. Wang, W. B. Capra, P. Liedo, and J. R. Carey. 1997. "Early mortality surge in protein-deprived females causes reversal of sex differential of life expectancy in Mediterranean fruit flies," *Proceedings of the National Academy of Sciences* 94: 2762–2765.

Pletcher, S. D. 1999. "Model fitting and hypothesis testing for age-specific mortality data," *Journal of Evolutionary Biology* 12(3): 430–439.

Promislow, D. E. L., M. Tatar, S. D. Pletcher, and J. Carey. 1999. "Below threshold mortality: Implications for studies in evolution, ecology and demography," *Journal of Evolutionary Biology* 12(2): 314–328.

Rogers, Richard G., Robert A. Hummer, and Charles B. Nam. 2000. *Living and Dying in the USA: Behavioral, Health, and Social Differentials of Adult Mortality*. San Diego: Academic Press.

Stern, N., A. Hochman, N. Zemach, N. Weizman, I. Hammel, Y. Shiloh, G. Rotman, and A. Barzilai. 2002. "Accumulation of DNA damage and reduced levels of nicotine adenine dinucleotide in the brains of Atm-deficient mice," *Journal of Biological Chemistry* 277: 602–608.

Strehler, B. L. and A. S. Mildvan. 1960. "General theory of mortality and aging," *Science* 132: 14–21.

Suh, Y., K.-A. Lee, W.-H. Kim, B.-G. Han, J. Vijg, and S. C. Park. 2002. "Aging alters the apoptotic response to genotoxic stress," *Nature Medicine* 8: 3–4.

Tatar, M. and J. R. Carey. 1994. "Sex mortality differentials in the bean beetle: Reframing the questions," *American Naturalist* 144: 165–175.

Thatcher, A. R., V. Kannisto, and J. W. Vaupel. 1998. *The Force of Mortality at Ages 80 to 120*. Odense: Odense University Press.

Van Remmen, Holly, Walter Ward, Robert V. Sabia, and Arlan Richardson. 1995. "Gene expression and protein degradation," in Edward J. Masoro (ed.), *Handbook of Physiology: Section 11: Aging*. New York: Oxford University Press, pp. 171–234.

Vaupel, J. W. 1990. "Relative risks: Frailty models of life history data," *Theoretical Population Biology* 37: 220–234.

Vaupel, J. W., J. R. Carey, K. Christensen, T. E. Johnson, A. I. Yashin, N. V. Holm, I. A. Iachine, V. Kannisto, A. A. Khazaeli, P. Liedo, V. D. Longo, Y. Zeng, K. G. Manton, and J. W. Curtsinger. 1998. "Biodemographic trajectories of longevity," *Science* 280: 855–860.

Vaupel, J. W., K. G. Manton, and E. Stallard. 1979. "The impact of heterogeneity in individual frailty on the dynamics of mortality," *Demography* 16: 439–454.

Wilmoth, John R. and Shiro Horiuchi. 1999. "Do the oldest old grow old more slowly?," in B. Forette, C. Franceschi, J. M. Robine, and M. Allard (eds.), *The Paradoxes of Longevity*. Heidelberg: Springer-Verlag, pp. 35–60.

Yashin, A. I. and I. A. Iachine. 1997. "How frailty models can be used for evaluating longevity limits: Taking advantage of an interdisciplinary approach," *Demography* 34(1): 31–48.